HEAT TRANSFER TO SINGLE- AND DOUBLE-ROW STIRLING ENGINE HEATER TUBES

Mark Connelly
Mechanical Technology Inc.
Latham, NY 12

Göran Olsson
United Stirlin
Malmö, Sweden

ABSTRACT

As part of the Automotive Stirling Engine (ASE) Development Program* conducted by Mechanical Technology Incorporated, heat transfer tests were performed in order to choose a specific Mod II (second generation) Stirling engine heater head geometry and to examine the interactive effects between this engine's two rows of tubes. The results are compared to simulated Mod I geometry and the available literature. A test section having a row of concentric tubes with a barrier gas in the annulus and water flowing through the inner tube was used to simulate the heat transfer from the combustion gas to the Stirling engine's working gas. Five finless front row and two finned rear row geometries were tested, both individually and together, over a range of operating conditions. The results showed enhanced heat transfer for the Mod II Stirling engine heater head geometry as compared to the Mod I engine geometry. A more efficient Mod II rear row accounts for a 10 to 50% improvement in the number of heat transfer units (NTU).

Dimensionless heat transfer parameters were obtained and compared to the available literature. A single relationship between Nusselt and Reynolds numbers was found for the front row geometries. This relationship gives almost 50% higher Nusselt numbers than that predicted in the literature. It is speculated that this difference stems from a small amount of radiative heat transfer and the presence of combustion products rather than hot air.

IN THE STIRLING ENGINE, the function of the heater head is to effectively transfer heat from the hot combustion gas at near atmospheric pressure to the oscillating working gas. The heater head is the assembly of tubing joining the regenerator housings and the cylinder heads. The current heater head geometry for the ASE Mod I and Mod II engines uses fins on the rear row of tubes to equalize the heat flux of the two rows. The increased heat transfer resulting from the fin design compensates for the lower combustion gas temperature and the lower flame radiation at the rear row when compared to the front row.

The heater head combustion-gas side is basically a tube row in cross-flow. Kays and London (1)** and Zukauskas (2) provide data for banks of straight tubes containing several rows in cross-flow. Ward and Jewad (3) have published data for single rows of tubes, as have Bankston and Back (4). The latter describe an experimental program to determine the heat transfer characteristics of a specific Stirling engine heater head. The work by Bankston and Back, as well as the present study, utilizes high-temperature combustion systems which provide gas-to-tube-wall temperature differences on the order of 1000 K. This effort examines the effect of a second finned row and somewhat lower Reynolds numbers.

Design changes in different engine heater heads were evaluated using a double mantle row rig (DMR). This rig, designed by United Stirling of Sweden (USAB), has a double-wall tube arrangement with water flowing through the inner tubes and an almost stagnant gas mixture in the annulus.

Several significant changes in heater head fin and tube geometry were incorporated in the Mod II design based on MTI's Mod I experience. For example, the Mod II will use a single tube per fin instead of the triple-tube fin of the Mod I. The Mod II will incorporate reduced tube diameters and increased front tube spacing. The involute front tubes in the Mod I engine will be replaced by a straight, hairpin-type tube in the Mod II engine.

Testing was necessary to define the effects of these design improvements on heater head performance. The DMR rig was used to map the heat transfer properties on the combustion side of various test sections which were made to simulate engine heater head geometries. The results from the tests where the Mod II rear tubes were run with different front sections demonstrated that the same section might perform quite differently, depending on the front row type with which it was coupled. This led to an additional series of tests, where each section was tested individually in the rig in an attempt to identify any interactive effects.

TEST RIG AND TEST SECTIONS

A schematic of the test rig showing the flow paths and locations of major instrumentation is shown in Figure 1. Hot combustion gas is generated in the gas-fired, laminar-flame combustor and passed over the test section. The fuel is propane. The composition of the barrier gas (ranging from 100% air to 100% helium) determines the heat flux for a given heater tube temperature. Thus, constant tube temperatures can be maintained over a range of combustion gas flow rates without problems such as localized boiling. The calculation of combustion gas temperatures between and in front of the test sections is based on the composition and temperatures of the gas measured behind the test sections and the heat extracted by the water.

Figure 2 shows one front row section and one finned rear row section, as well as the frame that attaches them to the rig. Two different fin geometries were used. One is the geometry used in the Mod I Stirling engine and the other is the geometry for the Mod II

*Department of Energy Contract No. DEN3-32 administered by NASA Lewis Research Center.

**Numbers in parentheses designate references listed at end of paper.

engine. Of the five plain front row sections tested, one was of the geometry used on the Mod I Stirling engine and the other four were used to determine the impact of front row tube spacing on the Mod II Stirling engine heater head performance.

The sections are detailed in Table 1. The heat transfer area of the test sections corresponds to ≈10% of that available in the Mod I and Mod II engines. The fins are brazed to the tubes with high-temperature Ni-Cr alloy. The inner tube is 304 stainless steel with a 2.5-mm outside diameter and a 0.5-mm wall. The outer tube is Inconel 625. The two tubes extend out to separate manifolds on either side of the rig where flows and temperatures can be measured. The manifold/tube interfaces are sealed with braze or O-rings. A 0.20-mm spacer wire is loosely spiralled along the annulus to ensure concentricity.

The test rig is instrumented so that two test sections can be run simultaneously. The normal distance between the front-tube row and the rear-tube row is 18 mm. Each test section has a minimum of six thermocouples on the outside of selected tubes. The tubes with the thermocouples, and the location of the thermocouples on these tubes, are chosen to give a good representation of average tube temperatures. These thermocouples are shielded to prevent radiation loss and to ensure good thermal contact with the tubes.

The thermocouples were installed for the two rear-row test sections as seen in Figure 3. The fins were installed first, and then the thermocouples were placed in a notch in the fins. The thermocouples were shielded with nichrome.

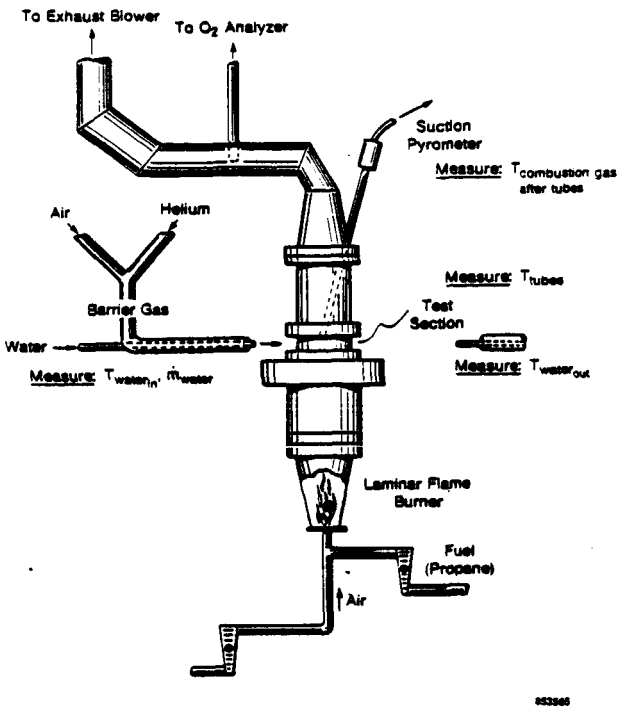

Fig. 1 - Double Mantle Row (DMR) Rig

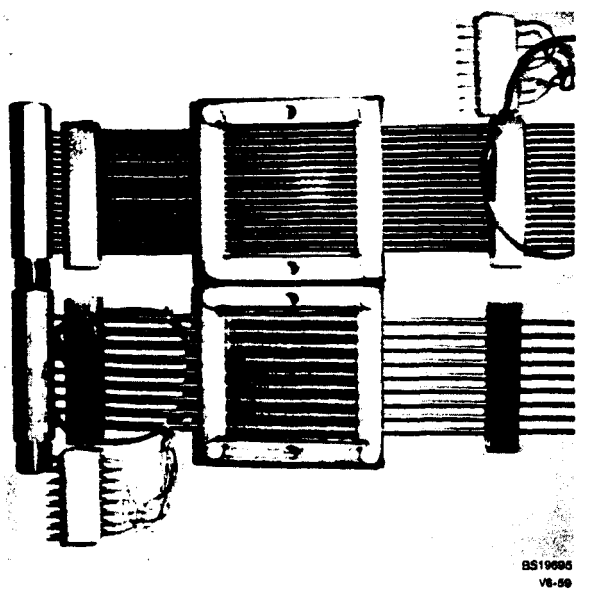

Fig. 2 - DMR Test Section Heater Tubes (Top, Plain; Bottom, Finned)

TEST PROCEDURE

The exhaust gas temperatures are measured by a suction pyrometer placed directly behind the rear tubes. This value is then corrected for suction efficiency. Suction efficiency is dependent on gas velocity: the higher the gas velocity past the thermocouple, the more efficient the measurement. Both a no-flow temperature and a maximum-flow temperature were read from the suction pyrometer.

For the tests with both front and rear test sections, front and rear tube temperatures were maintained at 800°C (±10°C) or the maximum attainable temperature at the low combustion-gas flow rates. Excess air (λ) was held constant at 1.35 (±0.05). The 800°C tube temperature is close to the engine design temperature of 820°C. The λ of 1.35 provides a flame temperature approximately equivalent to the Mod II engine design point. For the tests with single test sections, front and rear tube temperatures were maintained at 500°C (±20°C) and λ was held at 1.70 (±0.10). This was done to protect the test rig.

All tests were run over a propane flow range of 0.06 to 0.55 gram per second (g/s), which, if scaled to engine size, represents approximately 0.6 to 5.5 g/s of gasoline.

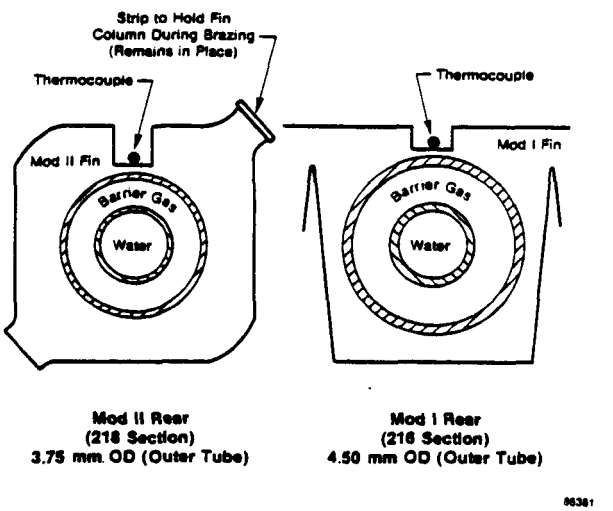

Fig. 3 - Thermocouple Placement for Rear-Row DMR Test Sections

Table 1 - Engine and DMR Test Section Geometries

Test Section Geometry (Front)

Section No.*	No. of Tubes n	Pitch (mm) P	OD (mm) D	Hydraulic Diameter (mm) D_h	One-Half Perimeter (mm) ℓ	Void Factor ψ	Tube Length (mm) ℓ_t	Flow Area (m^2) A_C	Heat Transfer Area (m^2) A_f
217	15	6.29	3.75	3.24	5.89	0.53	95.0	0.00363	0.0168
299	12	7.85	4.50	4.27	7.07	0.55	98.5	0.00396	0.0166
300	13	7.23	4.50	3.48	7.07	0.51	96.9	0.00344	0.0178
301	15	6.30	4.50	2.29	7.07	0.44	98.9	0.00267	0.0210
215	17	5.62	4.50	1.43	7.07	0.37	95.0	0.00181	0.0228

Test Section Geometry (Rear)

216	9	10.33	4.50	0.96	----	----	----	0.00266	0.110
218	12	7.62	3.75	0.64	----	----	----	0.00202	0.120

Mod II Engine Geometries (Front Tubes)

Configuration No. 1:	Configuration No. 3:
30 tubes/quad; Pitch = 5.69; OD = 4.16	25 tubes/quad; Pitch = 7.30; OD = 4.56

*Section No. 217, 299, 300, 301: Proposed Mod II; No. 215: Mod I; No. 216: Mod I style fins; No. 218: Mod II style fins.

All data were collected and processed on a Commodore 64 microcomputer. The temperature and pressure measurements were electronically sampled by the computer. Flow measurements and the oxygen content of the combustion gases were manually input via the keyboard. The computer was then used to calculate the NTU, the Nusselt number, the Reynolds number, and the convective heat transfer coefficients for the test sections at the actual fuel flow.

TEST RESULTS

The data obtained were very repeatable and had little scatter. Figure 4 shows representative data. Most of the graphs of NTU, Nusselt numbers and convective heat transfer coefficients are plotted versus the Reynolds number of the combustion gas past the test sections. The Reynolds and Nusselt numbers can use the hydraulic diameter, or one-half the perimeter, as the significant length parameter. Also, the velocity can be that between the tubes, or a reference velocity used in the literature (3) and defined as V_o/ψ^*. This latter velocity is the average value evaluated by integrating over the cylinder surface.

A least-squares, linear regression Fortran program was used in the analysis of all the data.

TESTS RUN WITH BOTH FRONT AND REAR SECTIONS - Assuming that both the front and rear test sections are at the same tube-wall temperature, the respective NTU values can be added to obtain an overall NTU for the heat exchangers as one unit. The sum of the NTU for the front and rear rows is plotted versus the combustion

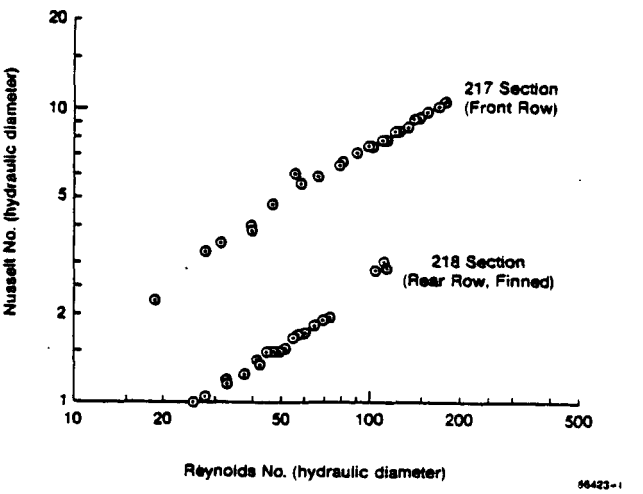

Fig. 4 - Representative DMR Test Data; Nu vs Re

*A nomenclature follows the CONCLUSIONS.

gas mass flow because the Reynolds numbers are different for front and rear rows at the same test conditions. The relatively large NTU values of the rear row predominate; the results are presented in Figure 5.

Front Tubes Run With Rear - The performance based on Nu_ℓ versus Re_ψ are all very close as seen in Figure 6. The Nusselt numbers for the test section with the smaller tube diameter (3.75 mm, section 217) were the highest. For the 4.50-mm tubes, the results indicate that a pitch of ≈7.2 mm is ideal, with performance dropping off on either side of this value.

Rear Tubes Run With Front - The results for the finned rear tubes are presented only as a function of hydraulic diameter. The Nu_{hyd} is strongly influenced by the hydraulic diameter. The relatively large hydraulic diameter of the Mod I (216) test section helps to provide it with a large Nu_{hyd} for a given Re_{hyd}, although the 218 section is still superior at higher Reynolds numbers (Figure 7).

The heat transfer coefficient is higher for the Mod II test section (218) because the different fin design provides more heat transfer area and directs the flow of the combustion gases towards the tubes.

TESTS RUN WITH ONLY ONE TEST SECTION - Figures 8, 9, and 10 highlight the results of running either the front or rear sections alone.

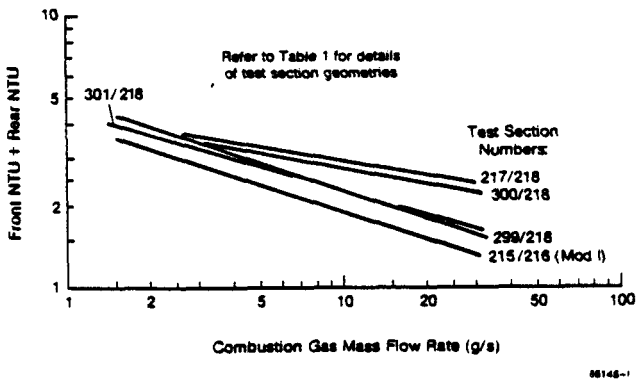

Fig. 5 - NTU vs Combustion Gas Mass Flow Rate; Front Row Plus Rear Row

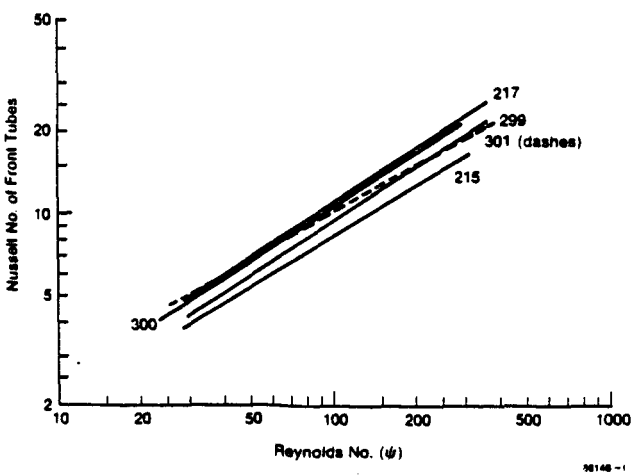

Fig. 6 - Nu_ℓ vs Re_ψ; Front Row When Run with Rear Row

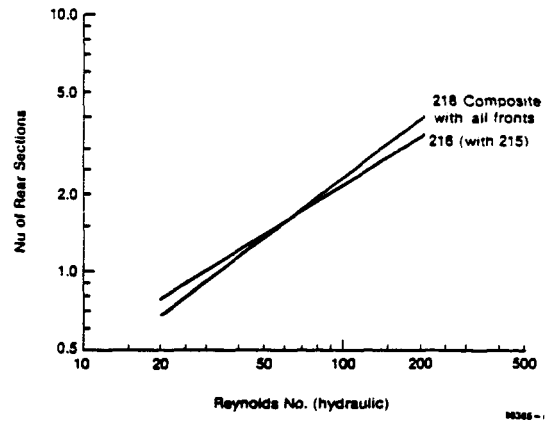

Fig. 7 - Nu vs Re_{hyd}; Rear Row When Run with Front Row

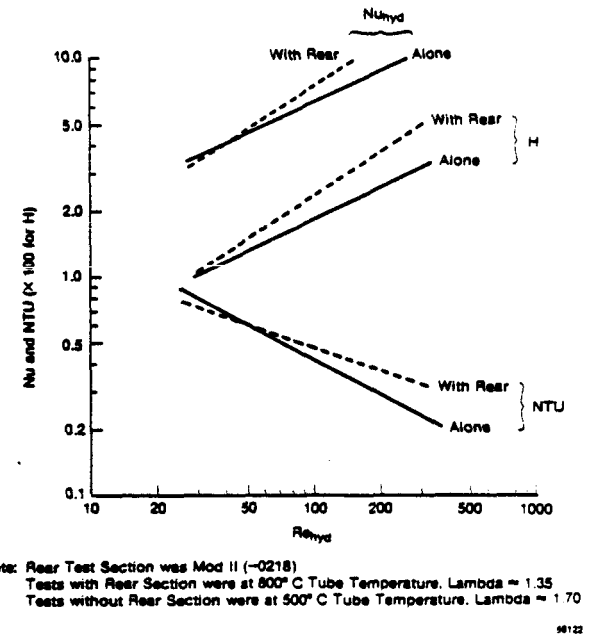

Fig. 8 - Comparison of NTU, Nu, and h; Front Section 217 (Least-Squares Fit of Data)

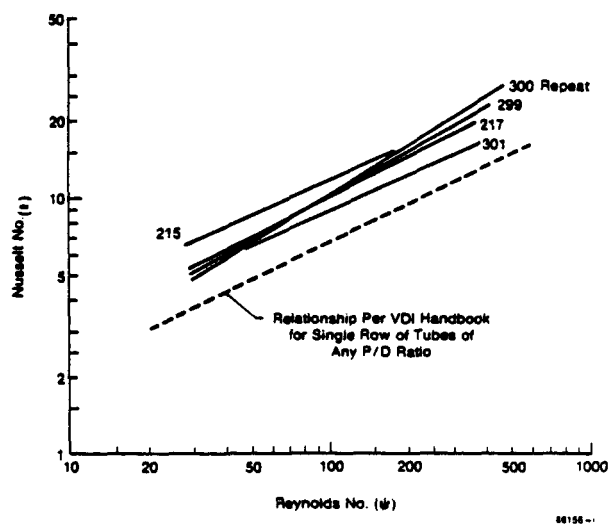

Fig. 9 - Nu_ℓ vs Re_ψ; Front Row Alone

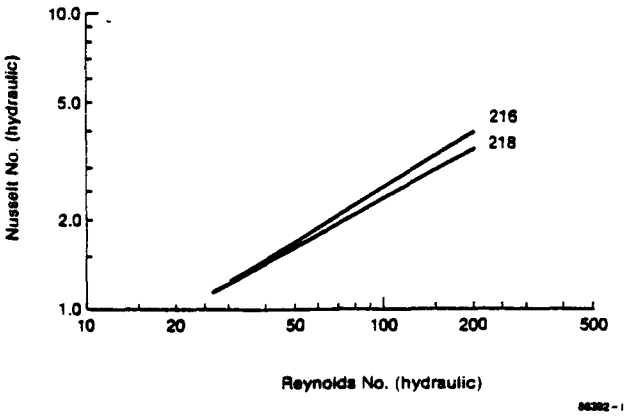

Fig. 10 - Nu vs Re_{hyd}; Rear Row Alone

Front Sections Alone - Figures 8 and 9 show a change to a less positive slope for all sections, when compared to tests coupled with the 216 or 218 rear section.

The biggest change seen in the Nu_ℓ versus Re_ψ is in the performance of the 215 section (Figure 9). There was a slight improvement in its performance at the lower Reynolds numbers when run alone. The reason for this is not clear, although it should be remembered that it was the only front row section coupled with the 216 rear section.

Rear Sections Alone - There was a performance increase in Nu_{hyd} versus Re_{hyd} (see Figure 10) at the low Reynolds numbers when the rear sections were run alone. The 216 section was slightly better than the 218 section when run without the rear section. The heat transfer coefficient of the Mod II was superior to Mod I. Improvements were made at the low Reynolds numbers when run alone.

DISCUSSION

In our discussion, we assume the following:

- Steady-state operation
- Constant overall heat transfer coefficient
- Uniform flow distribution through the tubes
- Uniform velocity and temperature profiles at entrances
- Negligible longitudinal conduction in walls and fluids
- No heat loss to the surroundings.

FRONT ROW NTU AND Nu - In Figure 9, the Nu_ℓ versus Re_ψ from all front row test sections run alone are plotted. A representative curve from the literature (5) is also shown in this figure. It is seen immediately that all curves cluster closely and that a single relationship between Nu_ℓ and Re_ψ can be used to describe the heat transfer characteristics of the test sections. The above is also true for the result from the runs where a front row was run together with a rear row (Figure 6). Furthermore, if the results from all runs with the front row are plotted, it is seen that the curves still cluster (Re_ψ < 100), and that the same relationship between Nu_ℓ and Re_ψ can be used in this range whether or not there is a rear row.

This relationship is

$$Nu_\ell = 0.711\ (Re_\psi^{0.574})$$

where $20 \leq Re_\psi \leq 100$.

This means that the rear row has only a small impact on the front row at lower Reynolds numbers, although this impact increases with an increase in Re. Our tests show a higher Nu_ℓ for the same Re_ψ than reference 5. This is explained by a small radiation contribution from the flame, from the hot combustion gases, and possibly from the surrounding walls of the test rig, whereas reference 5 cites only the convective contribution.

The small change in front row performance, when comparing tests with front and rear test sections to front sections alone (compare Figures 6 and 9), was due to the decreased turbulence on the back side of the front tubes. In the rig, there was a distance of 18 mm (or ≈4 to 5 diameters) between the front and rear tubes. However, because the second row was finned, there is significantly more turbulence generated than shown in the literature (3), and this turbulence increases the heat transfer on the back side of the first set of tubes. Note that the heat transfer coefficients are reduced only at higher Reynolds numbers for the tests with front sections, when compared to tests with front and rear sections. This implies that the upstream turbulence generated by the rear rows becomes significant when Re > 100. In the Mod II engine, the centerline distance from the front to the rear tubes will be 40 mm.

REAR ROW NTU - In Figure 11, NTU versus Re (Re > 20) is plotted for the different runs with the 218 rear row. It is seen that the presence of a front row strongly affects the rear row performance in the range 20 < Re < 60. A front row with closely spaced tubes has a negative effect on the rear row in that the NTU is lower than with a front row with widely spaced tubes.

It is reasoned that the flow leaving the front row is in the form of jets - the smaller the tube spacing the stronger the jet. There is an area with turbulent flow between the jets, but the main flow is in the jets, as shown in Figure 12. These jets reach only a small portion of each fin in the rear row creating fin inefficiences and lowering the rear row performance. A test was run with test sections 301 and 218 together with a 20-mm spacer between them (total distance between rows equaled 38 mm). This test showed that the rear row performance increased when the spacer was used, due to greater diffusion of the jets as the distance increased. At Re_ψ > 60, the turbulence created by the rear row itself probably dominates over the jet effect of the front row.

For the present Mod I geometry, the performance was also less when the front row was present. A direct comparison between Mod I and Mod II (216 and 218) shows

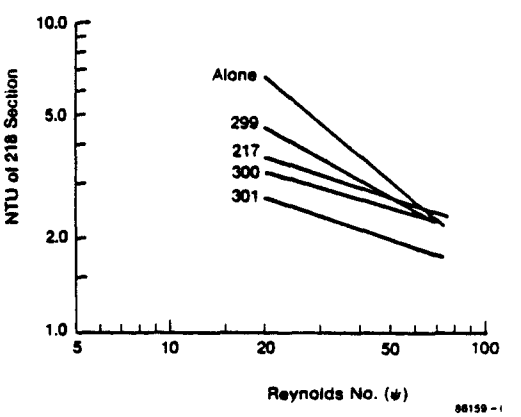

Fig. 11 - Comparison of Rear Row Performance (218) for Various Front Row Geometries and Alone

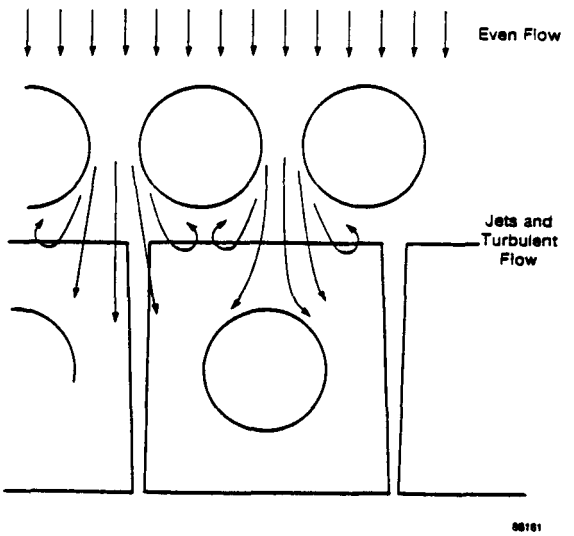

Fig. 12 - Front Row Effect on Rear Row

that the desired goal is reached, namely a better performing rear row for Mod II.

The decrease in performance of the rear row as the performance of the front row increases calls for another comparison to see if there is an optimum combination of the two rows. The comparison is made with the total NTU versus m_{cg} for the combined front and rear row runs (Figure 5). It is seen that all tested configurations of front and rear rows for Mod II will give a better performance than the present Mod I engine.

HEAT TRANSFER COEFFICIENT AND COMPARISONS TO COMPACT HEAT EXCHANGERS - One may wish to compare the results reported here and those available in the literature for compact heat exchangers. The designation of "compactness" is quite arbitrary but is usually taken as D_h less than 5.0 mm and heat transfer surface area density (β) greater than 700 m^2/m^3 (6). In our case, D_h was less than 5.0 mm for all test sections. β was in the range of 100 to 400 m^2/m^3 which doesn't meet the aforementioned minimum, indicating that some liberty was taken in comparing our results with compact heat exchanger literature. In addition, our Reynolds number regime is below that usually found in the literature.

For the Re regime of 300-15000, Figure 7-5 of Reference 1 and the equality

$$St = Nu/(Re \times Pr)$$

provides the relation

$$Nu = C_h Re^{.6} Pr^{.33}$$

For a longitudinal pitch of 1.00, the constant, C_h, and the equation reduces to

$$Nu = [0.5 \times (P/D) - 0.39] Re^{.6} Pr^{.33}$$

Using Figure 7-7 of Reference 1 which corrects for the number of tube rows, the equation is multiplied by 0.5 for a single row. If we assume a constant Prandtl number of ≈0.7, the equation becomes

$$Nu = [0.222 \times (P/D) - 0.1731] Re^{.6}$$

Also, knowing that $h = Nu \times (k/D_h)$, and approximating $k = 0.1$ W/(m°C), we have:

$$h = [1/(P-D)]\,[17.436\,(P/D) - 13.595] Re^{.6}$$

The predicted values for h would be as follows (all are versus Re_{hyd}):

- $h_{217} = 6.16 \times Re^{0.6}$
- $h_{299} = 5.02 \times Re^{0.6}$
- $h_{300} = 5.28 \times Re^{0.6}$
- $h_{301} = 6.01 \times Re^{0.6}$
- $h_{215} = 7.23 \times Re^{0.6}$.

These values are plotted in Figure 13, which can then be compared to the actual values. Note that the ranking of the sections based on equations from the literature agree quite well with the values reported from this testing. The actual values are higher than those reported in the literature, when extrapolated to higher Reynolds numbers.

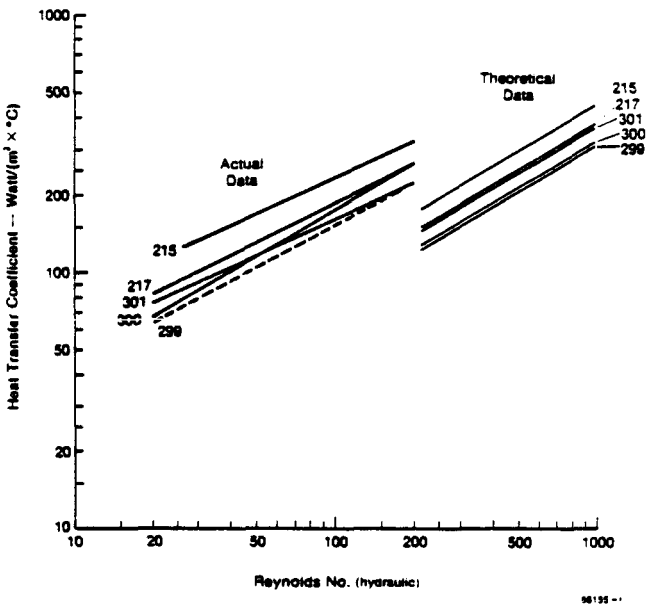

Fig. 13 - h vs Re_{hyd}; Front Row Alone

CONCLUSIONS

The results were compared to results available in the literature (1,5). It was seen that our Nu$_\ell$ numbers were ≈50% higher than those given in these references for a single row of plain tubes. This is due to radiation exchange with the flame and the surroundings and the presence of combustion products rather than hot air.

For the rear row, no single relationship was found from the tests owing to significant geometrical differences and the fact that only two test sections were used. However, it can be deduced that the influence of the front on the rear row makes it necessary to perform tests on each actual configuration and that in these tests the appropriate distance should be maintained between the two rows. The latter recommendation was not fulfilled in our tests and this makes it difficult to give any absolute numbers on the rear row NTU for the Mod II heater head. It is suggested that the NTU for the front and rear rows, respectively, be taken from the tests where two rows were run together.

Further testing is needed to find the influence of the distance between front and rear row and to find the relationship between the rear row NTU and its geometry.

The heat transfer properties of the Mod I and a range of possible Mod II heater tubes and fin designs were mapped. Mod II designs were shown to be superior